

## Evaluation of multi-scale representation of ocean flow fields using the Euler method based on map load

Bo Ai, Yanmei Liu, Zhenhua Wang & Decheng Sun

To cite this article: Bo Ai, Yanmei Liu, Zhenhua Wang & Decheng Sun (2019): Evaluation of multi-scale representation of ocean flow fields using the Euler method based on map load, Journal of Spatial Science, DOI: [10.1080/14498596.2018.1509739](https://doi.org/10.1080/14498596.2018.1509739)

To link to this article: <https://doi.org/10.1080/14498596.2018.1509739>



Published online: 17 Jan 2019.



Submit your article to this journal [↗](#)



Article views: 9



View Crossmark data [↗](#)



# Evaluation of multi-scale representation of ocean flow fields using the Euler method based on map load

Bo Ai<sup>a</sup>, Yanmei Liu<sup>a,b</sup>, Zhenhua Wang<sup>a</sup> and Decheng Sun<sup>a</sup>

<sup>a</sup>College of Geomatics, Shandong University of Science and Technology, Qingdao, China; <sup>b</sup>Urban Planning and Design Institute of The West Coast New Area of Qingdao, Qingdao, China

## ABSTRACT

This paper takes the map load as the evaluation indicator for multi-scale representations of ocean flow fields using Euler method. First, the map load of the ocean flow fields is calculated and the suitable map load interval is analysed in order to obtain the key scale for the multi-scale representation of ocean flow fields. Then, the load is limited by appropriate load intervals to fit the relationship between map load and scale. Finally, a mathematical model for multilevel comprehensive evaluation in fuzzy mathematics is established, and the usability of the resulting ocean flow field map is evaluated using questionnaires.

## KEYWORDS

map load; ocean flow fields; key scale; multi-scale representation

## 1. Introduction

Ocean current is an important dynamic marine phenomenon and a process that constrains a variety of other physical, chemical, biological and geological processes in the ocean. Ocean currents have a significant impact on the formation and change of climate, weather over the ocean and marine transportation (Silva *et al.* 2016). Ocean flow fields span a large range of scales, from small-scale coastal flows and surges, to mesoscale vortices, ocean fronts and even to long-term periodic oscillations at global scales (such as the El Niño phenomena) (Dai *et al.* 2014). The Euler method is a particularly common drawing method used to map ocean currents for these ocean flow field characteristics. In this method, sampled flow field data such as flow direction and velocity are represented by discrete arrow symbols, which can be used to realize the multi-scale visualization of the flow field (Brewer and Buttenfield 2006, Chen 2011).

Multi-scale representation of ocean flow fields using the Euler method face a key issue in that it is difficult to determine the specific scale when simplifying or densifying data. Existing basic electronic maps typically use key scales that are selected based on continued summary of accumulating experience and repeated practice, without support or guidance from a quantitative model. Unsuitable key scales have been found to result in worse user experiences and higher perceived cognitive workload (Jia 2002, Kiefer *et al.* 2017). In addition, unsuitable key scales can cause confusion and congestion of map symbols when zooming, which can result in a loss of geographic context (Huang *et al.* 2016).

Map load is a measure of the total amount of symbols and annotation within the map border and can be used to quantify the specific content contained in the map. Too many symbols will cause the map load to exceed the human visual tolerance threshold, which makes the map harder to read. Hence, map load is an important standard to consider in map content selection (Brewer and Buttenfield 2007). Therefore, in order to ensure the stability of the Euler method at different scales and analyse the suitability of key scales for simplifying or densifying data, this paper takes the map load as the evaluation indicator for such representations.

This paper chooses the linear symbol calculation method to obtain the map load, takes it as the evaluation indicator for map content selection, analyses the appropriate load interval for the map, fits the curve to calculate the key scale of multi-scale representation and finally evaluates the resulting map.

## 2. Map load calculation for the Euler method

In recent years, many experts and scholars have proposed a variety of electronic map load calculation methods. Meng (1985) proposed using the sum of the superposition of each colour of the map to obtain the map load. Jia (2002) suggested a method to calculate the map load of an electronic map area based on HLS colour difference, which takes the colour difference between target and background as the weight. However, methods focused on colour differences depend on psychological research which is prone to error. Harrie and Stigmar (2007) evaluated measures for quantifying the complexity of a map, and Harrie and Stigmar (2009) summarized measures for describing map readability. Deng and Wang (2010) came up with a model of screen saturation based on region partitions, but this algorithm is difficult to implement. Jiang *et al.* (2013) proposed a method based on RGB feature extraction; however, this algorithm is not appropriate when the background and the colour of the elements change. Sun and Jiang (2014) proposed a computational model based on map symbols, but its efficiency needs to be improved.

The arrow is the main symbol in a map of ocean flow fields. Arrows can symbolise natural, social and economic things with moving properties, focusing on direction, route, velocity, strength and so on. When used to illustrate the movement laws of seawater, the size of arrow symbols is typically related to the speed of the current, with larger arrows denoting faster currents (Zhang *et al.* 2001). Since, in the Euler method, the spatial regions represented by each arrow are all the same size, this paper counts arrows of different sizes as though they were symbols of the same size while calculating the number of pixels in each arrow symbol element. When calculating the map load, this paper counts the size and number of arrows and calculates the average size of the arrow symbol. This paper uses the map-symbol-based calculation method proposed by Sun, which obtains the area of the arrow symbol, and then converts it to the number of screen pixels before calculating the map load.

In ocean flow field mapping, the arrow symbols are only located in the ocean, which means the land area should be removed from the base map. This method divides the existing land vector file into small grids and calculates land area in the visual range. When calculating base map area, land area is subtracted from total area to get the

effective area of the base map. (This paper uses two different scales of flow field data: the large-scale precision is 0.0333°, and the small-scale precision is 0.5°.)

(1) Number of base map pixels

$$L_{bm} = \frac{BmH * k_1}{pscale} \tag{1}$$

$$W_{bm} = \frac{BmW * k_1}{pscale} \tag{2}$$

$L_{bm}$  is the length of the base map converted to centimetres,  $W_{bm}$  is the width of the base map converted to centimetres,  $k_1$  is the coordinate unit conversion parameter and  $pscale$  is the base map scale.

$$C_{bm} = (L_{bm} * k_2) * (W_{bm} * k_2) \tag{3}$$

$$C_o = C_{bm} - C_l \tag{4}$$

$C_{bm}$  is the total number of pixels in the base map screen,  $k_2$  is the number of pixels converted by the unit length,  $C_o$  is the number screen pixels of ocean in the base map and  $C_l$  is the number of screen pixels of lands.

(2) Number of arrow pixels

$$C_{ar} = A_l * k_2 * A_w \tag{5}$$

$C_{ar}$  is the number of arrow pixels,  $A_l$  is the length of the arrow symbol,  $A_w$  is the width of the arrow symbol, and  $k_2$  is the unit length conversion pixel parameter.

(3) Map load calculation formula:

$$L_a = \frac{\sum C_{ar}}{C_o} * 100\% \tag{6}$$

$L_a$  is the map load,  $C_{ar}$  is the pixel area occupied by the  $i$ th arrow and  $C_o$  is the area of the screen.

### 3. Suitable map load for ocean flow fields

Determining the appropriate load for a given map is a critical process which depends on the usage and scale of the map, as well as conditions in the mapped region (Yuan 2014). This process is especially complicated for electronic maps which can be scaled dynamically by the user, since the appropriate map load may change dynamically as the map scales. However, the main symbols used in ocean flow maps built on the Euler method are simply arrows which implicitly represent information such as the direction and velocity of ocean currents. Hence, when calculating map load, we need only calculate

the percentage of the base map area that is occupied by the arrow symbols. This in turn means that the appropriate map load changes little between scales.

Figure 1 shows how map load changes with scale, using consistent sampling data intervals. It shows that the map load increases as scale decreases. (In Figure 1 and below, the horizontal axis is the scale denominator divided by 10 million.)

Since user experience is subjective, this paper uses the expert scoring method to determine the suitable map load for the flow field. This process requires a series of flow field maps with the same scale and different data resolutions in the same area. This method includes inviting experts in the marine field to mark the map in order to determine the suitable load for the map. This section collates statistics representing the experts' scoring results and determines the appropriate map load corresponding to the maximum expert score.

First, several flow field maps were drawn using different map loads at a scale of 1:50,000,000 representing an area in the Atlantic ocean (Figure 2). Then the scores of the evaluation experts were collated (Figure 3), where the horizontal axis represents the map load and the vertical axis indicates the experts' scores for each of the six maps. We consulted experts and recorded their opinions, then determined that the appropriate load should be somewhere in the range between 18 and 28. When drawing the arrows, we adjusted the arrow density distribution so that the load for each map stayed within the appropriate load range. If the value of map load is more than 28 or less than 18, the map should be re-adjusted.

#### 4. Analysis of key scales for generalization

Multi-scale representation of ocean flow fields requires that the map on the screen is always clear, readable and appropriate at arbitrary scales (Jiang *et al.* 2010). Due to the interactivity and dynamic nature of electronic maps, they do have fixed scales. This

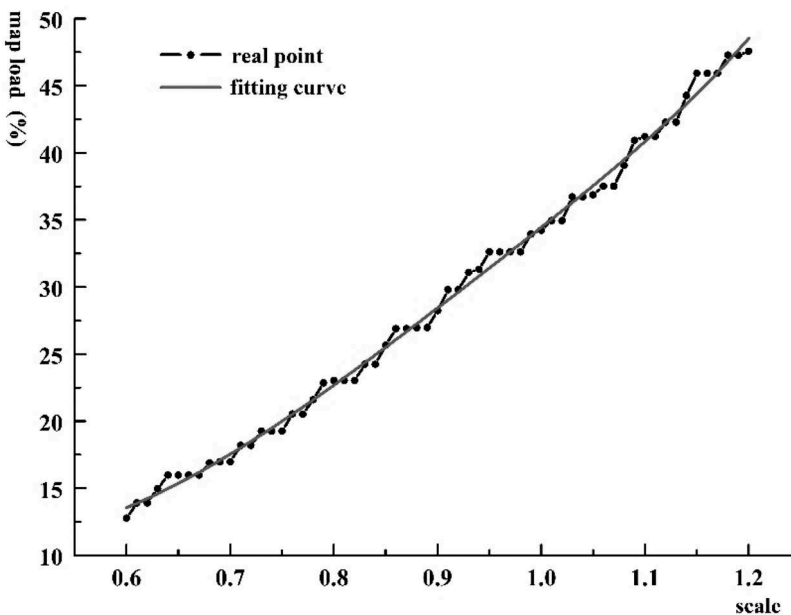


Figure 1. Diagram of map load and scale with thinning step length of 1.

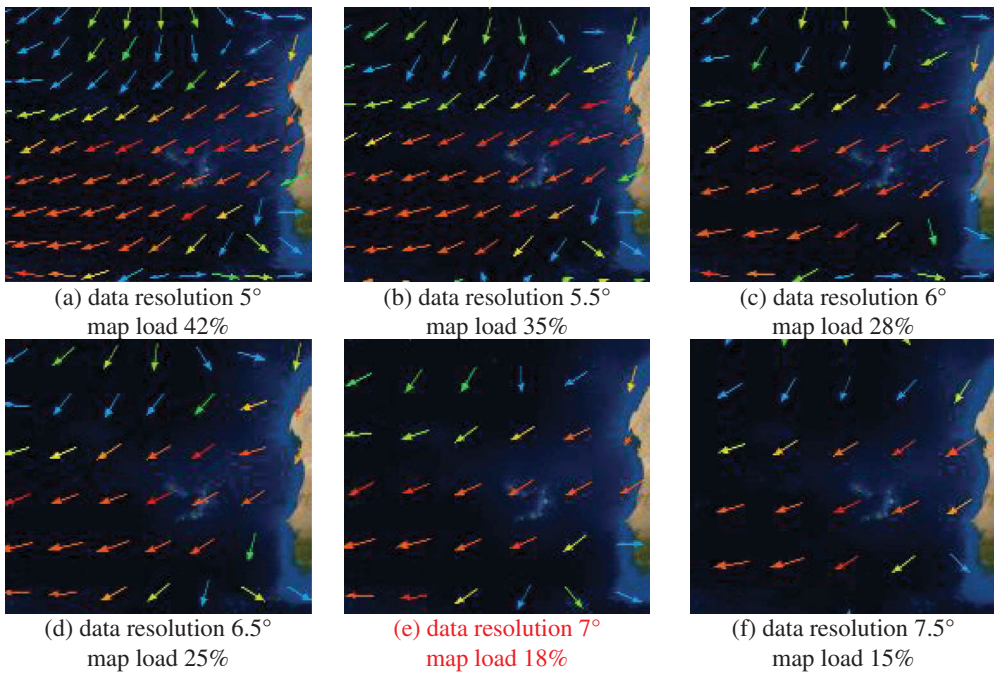


Figure 2. Different map loads under the same scale.

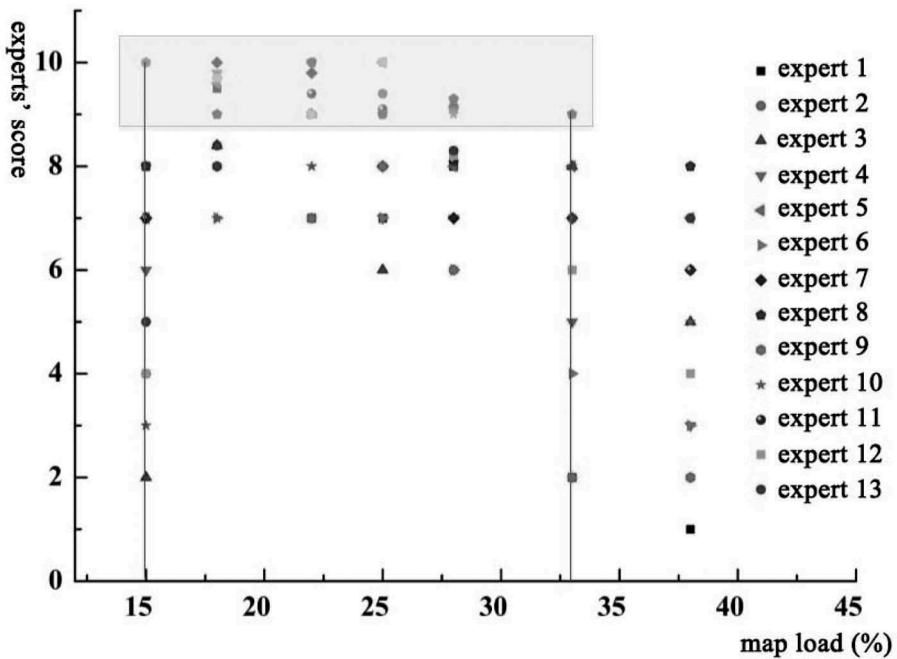


Figure 3. Expert scoring chart.

means that electronic maps can zoom steplessly. Owing to the constancy of human visual perception and map usage, there is no need to select, simplify, generalize and displace the content for each zooming increment. Rather, generalization takes place only when graphics zoom to a certain extent. The key scale is defined to be the screen scale that determines this extent (Brewer and Buttenfield 2010). To obtain the key scale for multi-scale representations of ocean flow fields, it is necessary to simplify or densify the spatial targets to reduce or increase spatial information to meet human visual readability and cognitive requirements.

#### 4.1. Analysis of key scales for the Euler method based on map load

The appropriate map load range places limits on the map load value, which means that the interval at which data are simplified on the map should be adjusted to ensure that the map will always remain within the appropriate load range. In this section, we discuss the adjustment of that interval, and then analyse the relationship between the electronic map load and small and medium scales by curve fitting to obtain the key scale. In the process of adjustment, however, we discovered that the map load cannot be guaranteed to be within the appropriate load interval at any scale, which is shown in Figure 4.

As seen in Figure 4, a simplifying step length of 1 causes overcrowded arrow symbols, while a simplifying step length of 2 causes overly sparse arrow symbols in the scale range between 0.9 and 1.4. This means that the map load in this range is unstable, and that adjusting the step length between any of these scales will result in a pronounced visual jump. This illustrates that both sides of the adjustment need to be taken into consideration when making adjustments to ensure that the map load is close to the appropriate range.

This paper fits the functional relationship between the scale, which is treated as the independent variable, and the map load, which is the dependent variable. The curves  $f_1(x)$  and  $f_2(x)$  are obtained by fitting the curve with simplifying step length of 1 and simplifying step length of 2, respectively. Figure 5 shows the fitting results. In order to ensure the map

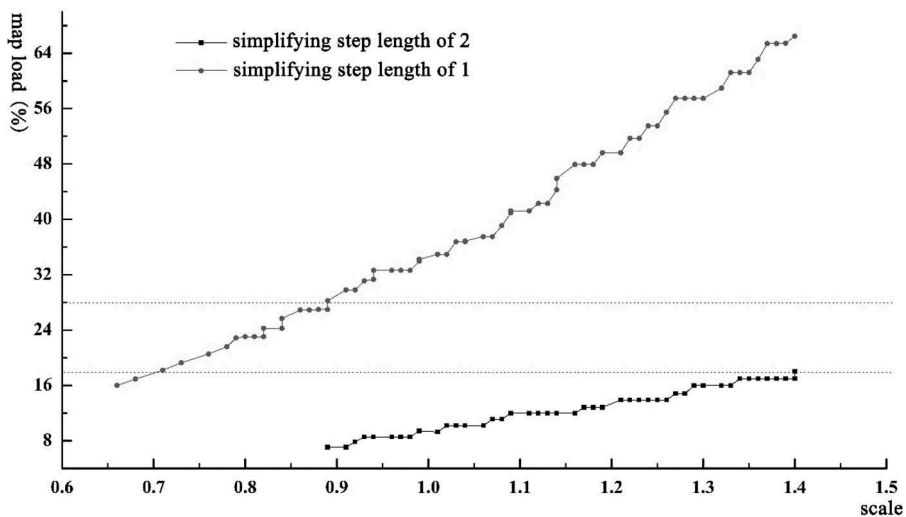


Figure 4. Comparison of map load change with different data intervals.

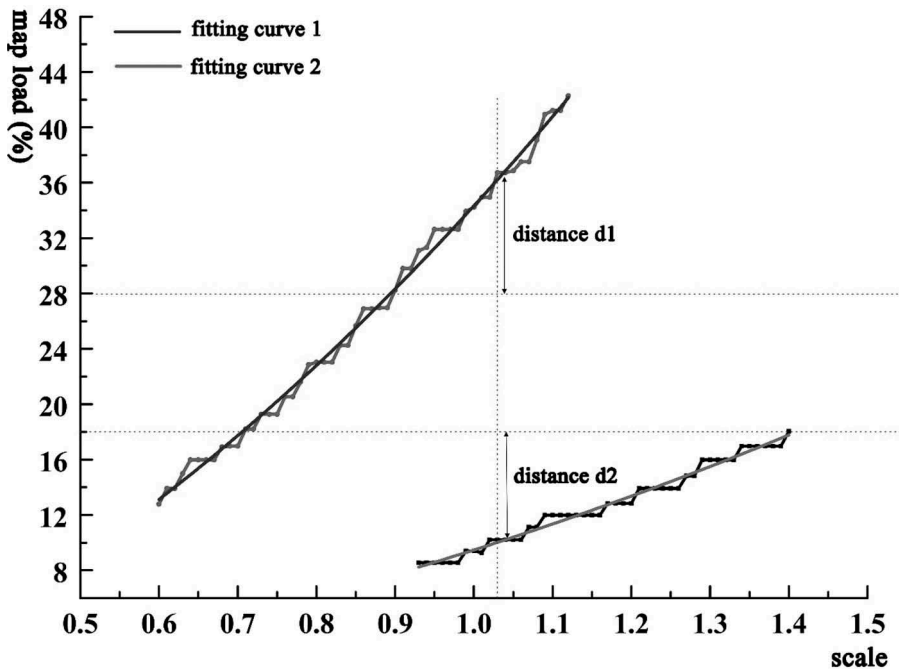


Figure 5. Fitting curve and key scale.

loads of both sides are close to the appropriate loads, we set the distance  $d_1$  from the fitting curve  $f_1(x)$  to the upper limit value of the appropriate interval to be equal to the distance  $d_2$  from the fitting curve  $f_2(x)$  to the lower limit value of the appropriate interval, and then obtained the calculated scale. When the simplifying step size is 1, the calculated scale is 1.03 million.

#### 4.2. Results of analysis of key scales

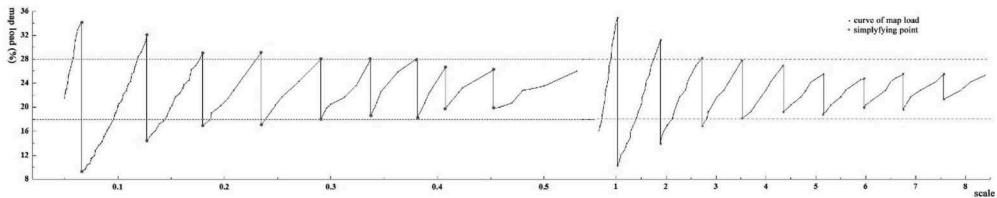
The scale range used in this study spans from 6 million to 80 million. While the scale is less than 65 million, both sides of the simplifying scale are within the appropriate load interval. In this section, we summarize the key scale according to the scale interval, simplifying step and corresponding data precision. Table 1 shows the key scale and the data resolution (note: the scale unit in the table is 10 million). Scales and map load at different simplifying intervals are summarized in Figure 6. When drawing maps of flow fields, the data resolution of different scales can be used.

### 5. Evaluation of multi-scale map

This paper calculates the key scale for simplifying ocean flow field data based on map load and summarizes the resolution of a flow field map under different scales in order to realize the multi-scale representation of flow fields. Then this paper needs to evaluate and analyse the map quantitatively. In order to verify the usability of the multi-scale representation of flow fields, this section evaluates the results of multi-scale representation. There are many factors to consider when evaluating the quality of thematic maps, and it is appropriate to

**Table 1.** 0.0333° and 0.5° data for each key scale.

Scale interval	Simplifying step	Data resolution
0.07	1	0.0333°
0.07–0.13	2	0.0666°
0.13–0.18	3	0.0999°
0.18–0.24	4	0.1332°
0.24–0.29	5	0.1665°
0.29–0.34	6	0.1198°
0.34–0.38	7	0.2331°
0.38–0.41	8	0.2664°
0.41–0.45	9	0.2997°
0.45–0.53	10	0.333°
~ 1.03	1	0.5°
1.03–1.89	2	1.0°
1.89–2.72	3	1.5°
2.72–3.54	4	2.0°
3.54–4.35	5	2.5°
4.35–5.15	6	3.0°
5.15–5.96	7	3.5°
5.96–6.75	8	4.0°
6.75–7.56	9	4.5°
7.56–8.42	10	5.0°

**Figure 6.** Load chart for different scales.

use the multi-level comprehensive evaluation method of fuzzy mathematics to establish the mathematical evaluation model.

### 5.1. Maps of multi-scale representation

First, a series of multi-scale maps of flow fields were constructed based on map load. Figure 7 shows the maps, including three maps of the Bohai region with high resolution of 0.0333° and three maps of the Pacific region with resolution of 0.5°.

### 5.2. Evaluation of multi-scale representation maps

The multilevel fuzzy comprehensive evaluation model divides the factors into several categories, and then makes a comprehensive evaluation on each class before finally evaluating the higher-level classes thoroughly according to the results of the evaluation (He 1984, Harrie and Stigmar 2010).

#### 5.2.1. Evaluation of the quality of flow field maps by the fuzzy multilevel comprehensive evaluation method

**5.2.1.1. Determine the set of evaluation factors A.** Set the factor set  $A = (A_1, A_2, \dots, A_n)$ , which is the first factor affecting the quality of the map. The first-level factor can be

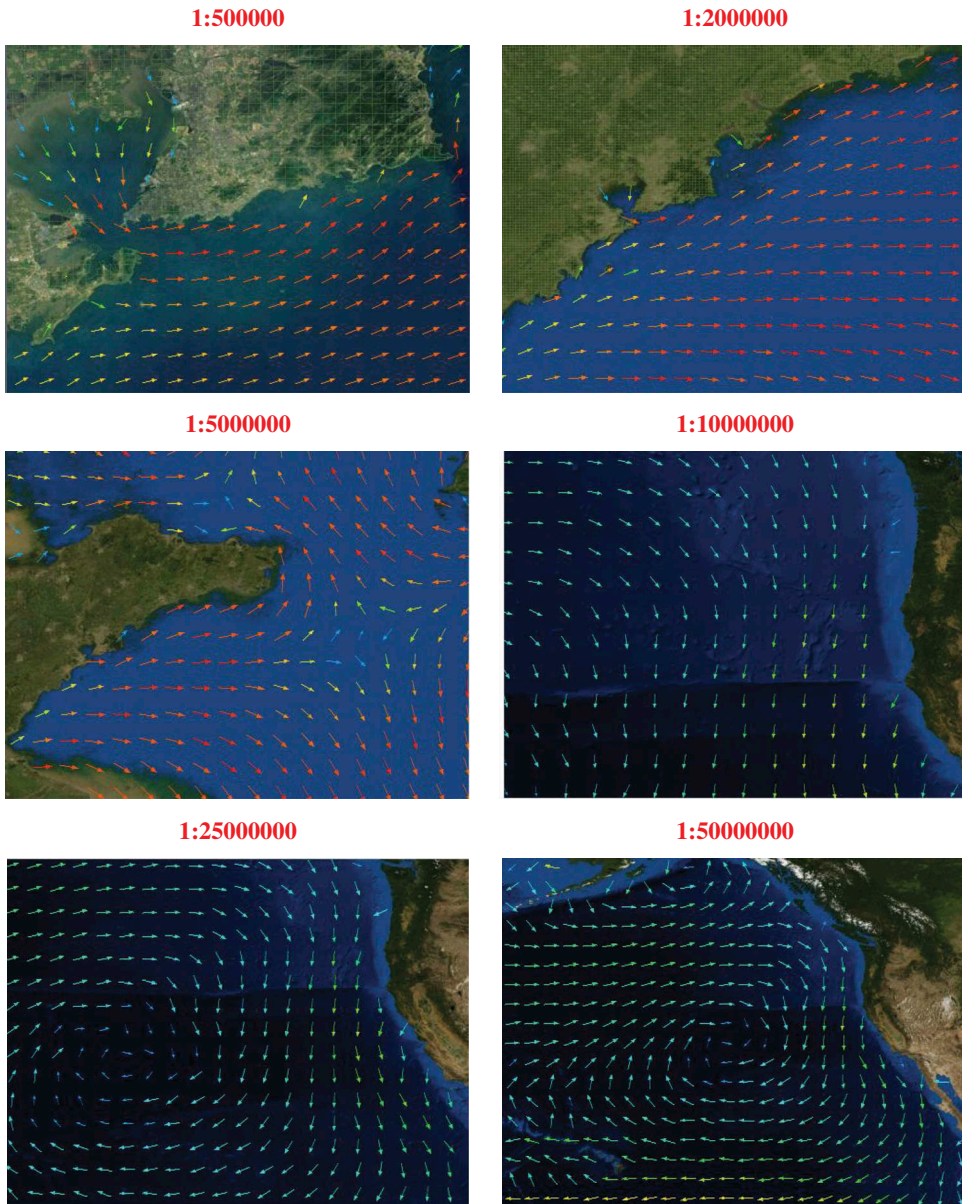


Figure 7. Multi-scale map of ocean flow fields.

evaluated synthetically by other factors of the second level; the second-level factor can be evaluated synthetically by other factors of the third level. In turn, the factor set  $A$  lists the second, third factors according to certain attributes and levels.

**5.2.1.2. Determine the evaluation level set  $V$ .** Suppose that the quality of map has  $n$  levels: what should be paid attention to is that the number of evaluation grades for each factor should be equal.

**5.2.1.3. Determining factor weight set.** Let the weight set be  $W = (W_1, W_2, \dots, W_n)$ , which can be estimated by means of various methods, such as asymmetric fuzzy relation analysis. The sum of the weight coefficients  $W = (W_1, W_2, \dots, W_n)$  meets the following condition:  $\sum_{i=1}^n W_i = 1$  ( $W_i \geq 0$ ).

**5.2.1.4. Determining fuzzy evaluation matrix  $R$ .** Assuming that the evaluation factors are divided into three levels, the fuzzy relational matrix of the third-level evaluation factors is different from those of the first and second levels.

- (1) This paper uses the scoring method to ensure the membership of the final factor to the comment  $V$ , and then counts the membership frequency of all evaluation personnel, which is taken as its fuzzy matrix.
- (2) The other-level fuzzy matrix  $R$  is created by combining the weight  $W$  with its next-level fuzzy matrix  $R$ , which can be expressed as  $W \times R$ . In addition, according to the principle of the maximum membership degree, the results of the evaluated units are determined.

### 5.2.2. Establishing a mathematical model for evaluating the map of flow fields

This paper analyses the contents and characteristics of the map, and then establishes the map quality evaluation indicator system, adopting the user classification survey and the multi-level fuzzy evaluation method to evaluate synthetically the usability of a multi-scale ocean flow field map.

#### 5.2.2.1. Establishing the weight of each indicator and evaluation indicator system.

Since the electronic map quality evaluation indicator system covers a wide range of contents, it is difficult to quantify the weights for each indicator. In order to ensure scientific rigour, rationality and precision of the weight calculation, we determined the weight set of the map evaluation indicator based on the characteristics of the map and the opinions of relevant domestic and international experts (Moghadam *et al.* 2015). The results are shown in [Table 2](#).

**5.2.2.2. Establishing evaluation level set  $V$ .** The evaluation level set ( $V$ ) is determined, and the quality of the map is divided into five levels: excellent ( $V_1$ ), good ( $V_2$ ), medium ( $V_3$ ), general ( $V_4$ ) and poor ( $V_5$ ). Namely:  $V = (V_1, V_2, V_3, V_4, V_5)$ .

**5.2.2.3. Evaluation calculation.** (1) First, this paper uses the scoring method to ensure the membership of the final factor to the comment  $V$ . While using a multi-level fuzzy comprehensive evaluation, this research uses a paper classification questionnaire. The results of any survey are more credible the higher the number of selected subjects. Therefore, we should select as many subjects as possible. Due to limited research conditions, we chose to select 100 participants, including 10 teachers of cartography, 24 students of cartography and geographic information systems and 66 students without any background in geographic information systems. [Table 3](#) shows the results of the questionnaire.

**Table 2.** Indicator system and the weight of each indicator.

Target layer	Criterion layer (weight)	Indicator layer (weight)
A Electronic map grade	C <sub>1</sub> validity indicators (0.44)	d <sub>1</sub> Integrity of map information (0.52)
		d <sub>2</sub> Clarity and aesthetic of map graphics (0.36)
		d <sub>3</sub> Representability of map graphics (0.12)
	C <sub>2</sub> efficiency indicators (0.30)	d <sub>4</sub> Map running speed (0.36)
		d <sub>5</sub> Accessibility of information (0.42)
		d <sub>6</sub> Interaction efficiency (0.22)
	C <sub>3</sub> satisfaction indicators (0.26)	d <sub>7</sub> Interface understandability (0.45)
		d <sub>8</sub> Operation complexity (0.55)

**Table 3.** Raw data of primary evaluation matrix.

Sub-factors	Excellent	Good	Medium	General	Poor
d <sub>1</sub>	41	37	15	5	2
d <sub>2</sub>	37	38	17	8	0
d <sub>3</sub>	35	40	18	6	1
d <sub>4</sub>	30	44	18	5	3
d <sub>5</sub>	43	38	12	6	1
d <sub>6</sub>	32	33	25	9	1
d <sub>7</sub>	21	52	19	6	2
d <sub>8</sub>	20	45	30	4	1

(2) Single-factor fuzzy evaluation: according to the survey data in Table 2, the single-factor evaluation matrix can be constructed directly from the membership degree of the final factor, e.g.  $R_{d1} = (0.41, 0.37, 0.15, 0.05, 0.02)$ . This paper constructs a single-factor evaluation matrix for  $d_1$  to  $d_8$ .

(3) First-level fuzzy comprehensive evaluation: the single-factor fuzzy evaluation matrix multiplied by the weight of indicator layer can produce a first-level fuzzy evaluation matrix. The method gets the weight coefficient of  $W_{C1}$  from Table 3, so that  $W_{C1} = (0.52, 0.36, 0.12)$ , then  $R_{C1} = (R_{d1}, R_{d2}, R_{d3}) * W_{C1} = (0.3064, 0.3032, 0.1308, 0.0520, 0.0076)$ .

(4) Multi-level fuzzy comprehensive evaluation: the first-level fuzzy comprehensive evaluation matrix multiplied by the weight of the criterion layer yields a multi-level fuzzy comprehensive evaluation matrix. The method obtains weight coefficients for A from Table 2,  $W_A = (0.44, 0.30, 0.26)$ , and  $W_A * (R_{C1}, R_{C2}, R_{C3})$  gives the final evaluation result  $R_A = (0.2806, 0.3418, 0.1511, 0.0528, 0.0115)$ .

(5) The normalized results of the multi-level fuzzy comprehensive evaluation of the map are shown in Table 4. Through map evaluation, the proportion of evaluations in the 'excellent' and 'good' groups is 62%. As a result, this map is quite reasonable.

## 6. Conclusions

Multi-scale representation can satisfy our cognitive needs when observing geographical phenomena that must be understood at a variety of scales. Multi-scale representations of ocean flow fields can help users understand the way that ocean water moves, from small coastal patterns to ocean-spanning currents. This paper studies the multi-scale representation of ocean flow fields in terms of map load in order to help satisfy the requirement of readability at a variety of different scales by controlling map load. The arrow symbol is used

**Table 4.** Multi-level fuzzy comprehensive evaluation results.

Evaluation grade	Percentage
Excellent	28.06
Good	34.18
Medium	15.11
General	5.28
Poor	1.15

as the object of a linear symbol calculation method to determine map load, and map load is used to analyse the key scale of the multi-scale representation. Finally, this paper evaluates the map through the multi-level fuzzy comprehensive evaluation method driven by a questionnaire survey, and shows that the map achieves satisfying results. However, in order to further improve map usability as well as the accuracy of our evaluation methodology, it is necessary to carry out further study on removing the land area from the base map and the map load calculation of arrow symbols.

### Disclosure statement

No potential conflict of interest was reported by the authors.

### Funding

This work was supported by The National Key R&D Program of China (No. 2017YFC1405006), The National Natural Science Foundation of China (No. 41401529) and A Project of Shandong Province Higher Educational Science and Technology Program (No. J15LH01).

### References

- Brewer, C.A. and Buttenfield, B.P., 2006. Mastering map scale: formalizing guidelines for multi-scale map design. In *Proceedings of AutoCarto*, 26–28 June 2006 Vancouver, Washington: Cartography and Geographic Information Society Gaithersburg, Maryland, 1–13.
- Brewer, C.A. and Buttenfield, B.P., 2007. Framing guidelines for multi-scale map design using databases at multiple resolutions. *American Cartographer*, 34 (1), 3–15. doi:10.1559/152304007780279078
- Brewer, C.A. and Buttenfield, B.P., 2010. Mastering map scale: balancing workloads using display and geometry change in multi-scale mapping. *Geoinformatica*, 14 (2), 221–239. doi:10.1007/s10707-009-0083-6
- Chen, J., 2011. Study on the intergrative organization and representation method for geographical entity in different scales. Thesis (PhD). Zhejiang University, China.
- Dai, C., et al. 2014. *Regional oceanography of Taiwan*. Taipei: Publication of National Taiwan University.
- Deng, H. and Wang, Y., 2010. A calculative model of screen saturation based on region partition. *Science of Surveying and Mapping*, 35 (3), 153–155.
- Harrie, L. and Stigmar, H., 2007. An evaluation of measures for quantifying complexity of a map. The JUMP project, <http://www.jump-project.org/> [accessed 04 04 2007].
- Harrie, L. and Stigmar, H., 2009. An evaluation of measures for quantifying complexity of a map. <http://drops.dagstuhl.de/opus/volltexte/2009/2137> [accessed 2009]
- Harrie, L. and Stigmar, H., 2010. An evaluation of measures for quantifying map information. *Isprs Journal of Photogrammetry & Remote Sensing*, 65 (3), 266–274. doi:10.1016/j.isprsjprs.2009.05.004

- He, Z., 1984. The principle of fuzzy mathematical multilayer symthatic evaluation and its' application of quality evaluation in thematic mapping. *Acta Geodaetica Et Cartographica Sinica*, 4, 266–276.
- Huang, L., et al., 2016. Engineering web maps with gradual content zoom based on streaming vector data. *Isprs Journal of Photogrammetry & Remote Sensing*, 114, 274–293. doi:10.1016/j.isprsjprs.2015.11.011
- Jia, F., 2002. *Research on the theories & methods of electronic maps' multi-scale representation*. Thesis (PhD). Information Engineering University. The China. doi: 10.1044/1059-0889(2002/er01)
- Jiang, N., et al., 2010. Establishment and application of multi-scale display model in basic electronic map. *Geomatics and Information Science of Wuhan University*, 35 (7), 768–772.
- Jiang, N., et al., 2013. A computational method of information load on electronic map based on RGB feature extraction. *Engineering of Surveying and Mapping*, 22 (6), 39–42.
- Kiefer, P., Giannopoulos, I., and Raubal, M., 2017. Controllability matters: the user experience of adaptive maps. *Geoinformatica*, 21 (3), 1–23. doi:10.1007/s10707-016-0282-x
- Meng, L., 1985. The quantitative methods of visual map load and its application. *Journal of Institute of Surveying and Mapping*, 2, 53–63.
- Moghadam, S.A., Karimi, M., and Mesgari, M.S., 2015. Application of a fuzzy inference system to mapping prospectivity for the chahfiroozeh copper deposit, kerman, iran. *Surveyor*, 60 (2), 233–255.
- Silva, M.C., et al., 2016. Numerical simulations of wave–current flow in an ocean basin. *Applied Ocean Research*, 61, 32–41. doi:10.1016/j.apor.2016.10.005
- Sun, Q. and Jiang, N., 2014. Research on electronic map load calculation model and its application. *Bulletin of Surveying and Mapping*, 9, 54–57.
- Yuan, K., 2014. *Modern cartography course*. Beijing: Publication of Science.
- Zhang, J., Hu, W., and Zhang, Y., 2001. Study on the dynamic graphic symbols in quantitative map. *Geo-Information Science*, 1, 77–80.